J Therm Anal Calorim (2016) 125:1411–1423
DOI 10.1007/s10973-016-5704-3

Investigation of key parameters influence on properties of the green pellets and lightweight ceramic proppants obtained by mechanical granulation method

J. Szymanska[1] · P. Wisniewski[1] · M. Malek[1] · J. Mizera[1] · K. J. Kurzydlowski[1]

Received: 26 October 2015 / Accepted: 12 July 2016 / Published online: 25 July 2016

Abstract Ceramic proppants are determined as material designed for hydraulic fracturing in the shale gas industry. Shale formation is fractured due to pumping the fracturing fluid including proppants into the unconventional well. Ceramic granulates set in the newly created fissures act as a prop and permit the shale gas of flowing up the well. The aim of this research was to study and compare ceramic materials used as proppants. The investigation includes four kinds of industrial proppants in green state obtained in a way of mechanical granulation process without binder and with poly(acrylic–styrene) dispersion in amount of 5 mass% with respect to the powder. Green pellets and afterward sintered granulates with 16/20 and 20/40 mesh were also analyzed and compared. Usefulness of green pellets was estimated basing on bulk density, thermal analysis, thermogravimetry, roundness coefficient and porosity results. Structure, morphology and chemical composition of the green state samples were determined by scanning electron microscopy with energy-dispersive spectroscopy. The sintered proppants were also characterized with X-ray tomography, turbidity and solubility in acid. Mechanical strength of these samples was established during subjection to crush test. The outcomes show a suitability of the studied material and prove chemical composition and grain size influence on the integrity of created fractures and therefore the extraction of the unconventional gas out of the well.

Keywords Ceramic proppants · Thermal analysis · Hydraulic fracturing · Shale gas

✉ J. Szymanska
joanna.szymanska.pl@gmail.com

[1] Faculty of Materials Science and Engineering, Warsaw University of Technology, Woloska 141 Street, 02-507 Warsaw, Poland

Introduction

Natural gas is one of the most important sources of energy on the global market that reduces CO_2 emissions more than twice in case of coal and 40 % lower than oil. A real and promising perspective for replacing conventional resources can be deposits of unconventional natural gas that occurs in shale [1]. This group of hydrocarbons, formed by resources trapped in impervious rocks, demands specific fracturing ways. Standard permeability of conventional deposits totals up 10^{-3} D (Darcy), while it is much lower on the scale for the shale gas (10^{-9} D) [2]. Actually, the unconventional reservoirs in the world prevail nearly twice over conventional gas. It is predicted that global shale gas extraction will increase from 13 % in 2009 up to 23 % in 2035 which is equal to 1.6 bln m^3 [3]. Predominant areas in mining industry are Asia, North and South America. Scale of European unconventional reservoirs is thrice smaller (Sweden (1.2 bln m^3), Ukraine (1.2 bln m^3), France (5.1 bln m^3), UK (5 bln m^3), Norway (2.4 bln m^3), Germany (7–22 bln m^3) and Poland (0.8 bln m^3)) where deposits occur twice deeper (up to 6 km) in comparison with US shales. Polish shale formations consist of quartz, loamy, silica, marly and bituminous rocks that determine more severe geological and geochemical parameters than American ones [4].

The most widely practiced and enhanced extraction technique is hydraulic fracturing with use of viscous liquid medium transporting suspended proppants [2]. Pumping such pressurized fluid into a wellbore generates fractures in the shale rock and thus free flow of hydrocarbons toward surface. The main component of fracturing liquid is water (90 %). The rest composes of proppants (9.5 %) and chemical substances (0.5 %) [5].

The great importance constitutes the proppants which act as eco-friendly material mainly used as a prop for

induced cracks; thus, the fractured rock cannot close when injection is stopped and pressure removed. Then, the permeable fissure allows the flow of gas to the well so that output of natural gas from reservoir is possible [5]. There are currently four types of proppant: quartz sand, resin-coated sand, bauxites and ceramic granules. The last ones demonstrate the most preferable parameters as uniform round shape and much higher strength than quartz sand and resin-coated sand. Such characteristics prove suitability for the fracturing of deep gas stratum with high closure pressure. Compared to the other propping materials, ceramic ones have superiority of smoother surface, higher fracturing strength and low solubility in acids [6].

Production of proppants has been launched in the early 50 s of the twentieth century where the pioneer material was the white quartz. In the 60 s, there ensued improvement of its strength with simultaneous reduction in its specific mass. Nowadays, the ceramic proppants are widely used to replace other proppant materials (natural quartz sand, fused zircon glass balls and metal balls), particularly in deep situated wellbores to increase output of gas by 30–50 % [7].

Polish extreme geological conditions in deep wells determine application of light ceramic proppants presenting the highest quality as thermal stability and crush strength [8]. Hence, there is a need of production of ceramic proppants with higher amount of Al_2O_3 than SiO_2 in order to obtain superior mechanical parameters [9]. It means these propping agents have to resist closure stress that surpasses 15,000 even to 20,000 psi–139 MPa (temperature up to 260 °C) [10]. Otherwise, the material will be crushed into fines that will block the permeability of a proppant over time. Five percentage of splinters affect reduced flow through the fractures by 60 % [11]. The strength in ceramic materials is also dependent on pores geometry, distance between pores, pore overlapping, distance between pores and surface [12]. Uniform size of proppants ensures a proper level of porosity and thus facilitated gas migration toward the wellbore for subsequent extraction [9]. Moreover, high roundness coefficient prevents loss of fracture width and thus enhances gas flow. Size of granules can vary between 8 and 140 mesh corresponding to sphere diameters (106 μm–2.36 mm]. Permeability lowers with the growth of proppant diameter. What is more, lower specific mass (~2 g cm^{-3}) reduces not only expenditures of the whole fracturing process but also proppants settling velocity and thus placement into fractures in larger concentration yielding [13]. Acids as HCl/HF mixture can be pumped down the hole to ensure demanded fracturing conditions. Proppants suspended in such environment should perform acid solubility resistance to prevent their size distribution. High HF concentrations result in increased proppants dissolvent [14].

Ceramic proppant is sintered mainly from bauxite mixed with silicate, kaolin and iron–titanium oxide that prove many works of Polish scientists [15–17]. However, in order to increase its mechanical strength, resistivity to solubility in acids and lower specific mass, polymer addition to the initial raw materials mixture is a common operation. Thermal analytical techniques seem to be useful to characterize their thermomechanical properties. Differential scanning calorimetry (DSC) is a versatile technique used for about three decades that permits quantitative and qualitative heat estimation that is taken or generated in materials phase transition processes related to phase change, melting, coagulation and other transitions connected with a heat flow. Moreover, thermal conductivity, thermal diffusivity, specific heat or thermo elasticity can be measured to provide quantitative and qualitative information about physical and chemical changes involving endothermic or exothermic processes or heat capacity change [18]. The critical parameter is a glass transition temperature (T_g) that determines thermal and dynamical properties and additionally the detection of impurities or unidentified admixtures of used polymers [19, 20]. In case of a drop of polymer temperature below T_g, there increases its brittleness. As the temperature rises above this critical value, the polymer becomes more rubber-like, which have been investigated in many studies [21, 22]. That is why, determination of T_g is a crucial issue in polymer selection for the proppants production.

What is more, the thermal degradation of these materials can be verified by thermogravimetry (TG). This technique is based on measurement of the temperature changes that occur in a substance as a result of chemical reactions or physical changes. The analysis is carried out by a sample weighing and continuous heating with constant rate. The mass change of a sample corresponds to the temperature growth that can be displayed as the thermogravimetric curve or the differential thermogravimetric curve (rate of mass loss versus temperature curve). The curves are the source of information about the thermal stability and composition of the examined sample, intermediates and wastes. Many works have been devoted to the application of this method [23–27].

Studies of light ceramic proppants obtained by mechanical granulation method basing of Polish raw materials will be contribution to improvement their properties and taking the lead on the global shale market.

Materials

Experimental samples of the proppants have been produced from white clay (1G, particle diameter ~40 μm), china clay-known as kaolin (1J, particle diameter ~40 μm) and bauxite (1B, particle diameter ~20 μm) that have been mixed in oscillatory and turret mills. Afterward, the

powder was subjected to granulation process in a turret granulator and drying in a spray dryer.

Among six mixtures, five of them were composed of 20 % poly(acrylic–styrene) dispersion (5 mass% with respect to the powder). The highest rotational speed of mixing was equal to 350 RPM. Two series from obtained raw proppants were sintered in a rotary kiln. During the first and second firing (lasting 4 h), sintering temperature amounted to 1200 °C (first firing) and 1240 °C (second firing), whereas in a loading zone it totaled up to 500 °C. The sintering exposition period averaged to 15 min, while speed of the kiln heating to the maximum temperature was 0.5 RPM. The final granulated product was fractionated in the sieves with proper mesh sizes.

Methodology

X-ray diffraction (XRD) measurements of the ground raw materials were taken out with *D8 Advance X-ray Bruker* based on the powder dispersing onto single-crystalline quartz sample holders and 30-min scan with 10–75° scanning spectrum. The aim of this experiment was crystalline phase estimation present in the raw materials and polymorphous forms distinction.

Moreover, milled raw materials and proppants sample specimens were subjected to investigate fracture surface, size and shape in SEM analysis with *HITACHI SU 8000* (Hitachi, Japan). The collected pieces were placed on pin-sample holders (1.5 cm diameter) using conducting double-sided tape. The microstructure characterization was carried out using BSE detector, voltage 5 kV, working distance 10.8 and 15.4 mm with magnification from 80 to 1000 times.

In order to estimate chemical composition by located particular elements, energy-dispersive spectroscopy (EDS) was applied with use of *Thermo Noran detector* combined with scanning electron microscope *Hitachi SU 8000.* Roentgen microanalysis enabled an accurate identification of surface topography by back-scattered electrons.

Roentgen tomography was conducted with use of *Roentgen Micro*tomograph *SkySkan 1742*. The proppant samples were scanned with 2000 px × 1000 px resolution in range rotation 0–180° (results registration every 0.4° with use of Al–Cu filter). Basing on scanning data, the results were subjected to reconstruction to obtain cross section. Every sample structure at x, y, z planes intersection was also analyzed in software in order to 3D models preparation.

Bulk density study enabled to estimate proppants mass required to unit volume filling. This parameter can change depending on how the material handling. In this case, an essential factor is also porosity. Bulk density determination allows to mass of proppants preparation needed to crack inlay during the shale gas extraction process and further storage of the propping material. The experiment was based on sleeve calibration (volume 150 mL) with a defined mass (m_{f+gp}) and then water pouring to its upper rim (mass determination m_{f+gp+l}). The sleeve volume V_t was computed according to Eq. (1):

$$V_t = \frac{m_w}{0.9971} / \mathrm{cm}^3 \tag{1}$$

where m_w, water mass (netto) from $m_{f+gp+l} - m_{f+gp}$/g; 0.9971/g cm^{-3}, water density at temperature 21 °C.

Further step was dry and empty sleeve weighting (m_p) and the same procedure in case of beaker completely filled with proppants (volume 150 mL, mass m_{f+p}). Hence, the bulk density ρ_{bulk} was obtained from Eq. (2):

$$\rho_{bulk} = \frac{m_p}{V_t} / \mathrm{g\ cm}^{-3} \tag{2}$$

where m_p, mass of proppants from $m_{f+p} - m_p$/g; V_t, sleeve volume/cm^3.

The degree of roundness was determined with use of *MicroMeter 1.04* program where proppants stereoscopic images (*Nikon DS-F12*) were analyzed. The granule diameter and their areas were used to roundness coefficient calculations according to Eq. (3):

$$W_k = \frac{4 \times \pi \times A}{L^2} \tag{3}$$

where A, surface area of proppant/mm^2; L perimeter of proppant/mm.

Turbidity estimation was carried out in order to determine amount of proppants particles suspended in a water solution according to PN-EN ISO 13503-2 norm. Increased turbidity level corresponds to growth of solid particles in a suspension. The measurement was conducted with use of *TurbiDirect_4a Turbidimeter* where a beam was directed perpendicularly to the detector track.

Solubility in acids was estimated according to PN-EN ISO 13503-2 norm. In the measurement, 5 g of proppants put in 100 mL of 12:3 HCl:HF solution (12 mass% HCl, 3 mass% HF) in a bath at 66 °C temperature for 30 min. The solubility in such acid solution indicates soluble compounds content (carbonates, micas, ferrous oxides, loams) present in the investigated material. The solubility S was obtained basing on formula (4):

$$S = \frac{(m_S + m_F - m_{FS})}{M_S} \cdot 100[\%] \tag{4}$$

where m_S, mass of the sample/g; m_F, mass of the filter/g; m_{FS}, mass of the dry filter with sample/g.

Thermal analysis of poly(acrylic–styrene) dispersion was carried out through differential scanning calorimetry analysis (DSC) with use of *TA Instruments DSC Q1000*

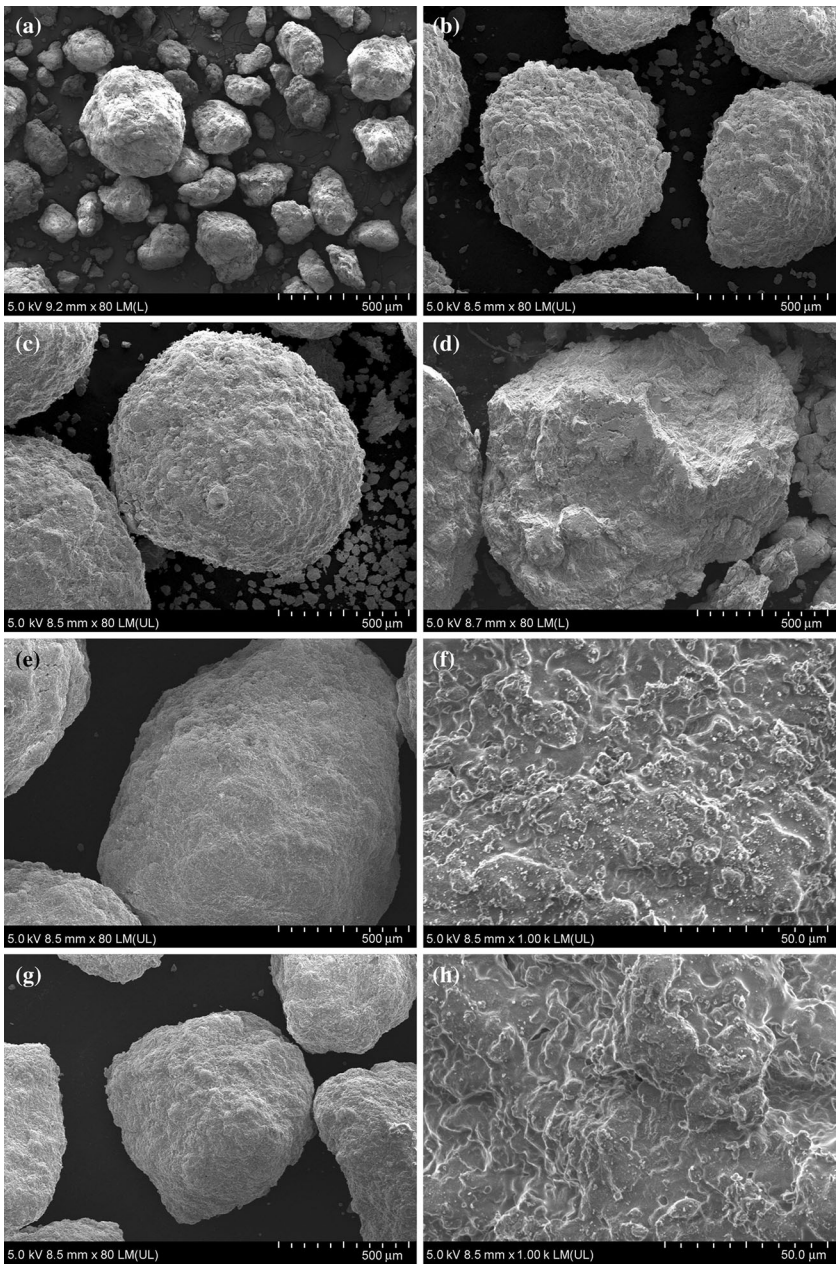

Fig. 1 SEM images of investigated proppants: **a** G1 green pellets, **b** 20/40 green pellets, **c** 16/20 green pellets, **d** G5 green pellets at ×80 magnification, **e** 16/20 sintered proppants with ×80 magnification, **f** 16/20 sintered proppants with ×1000 magnification, **g** 20/40 sintered proppants with ×80, **h** 20/40 sintered proppants with ×1000 magnification

apparatus. Temperatures characteristic for phase transitions and their enthalpy values were determined. Temperature calibration proceeded with use of indium model sample. Measurements were taken out in a nitrogen atmosphere. The samples with a mass of 10 mg were subjected to heating and cooling with a constant speed ($V_h = 10$ °C min^{-1}) in a temperature range from −40 to 100 °C.

The thermogravimetric (TG) and derivative thermogravimetric (DTG) curves for the polymeric dispersion were obtained due to analysis conducted using *TA Instruments TGA Q 500* under nitrogen atmosphere at a heating rate (V_h) of 10 °C min^{-1} from 20 to 800 °C. The sample initial mass was about 45.00 mg. The onset temperature of degradation (T_{onset}) was obtained by the intersection of the tangent of the peak with the extrapolated baseline from the first degradation peak of the TG curves.

Crush test was conducted of hydraulic press adjusted to exert pressure up to 15,000 psi. Amount of the proppant sample put in a cylinder was determined according to Eq. (5):

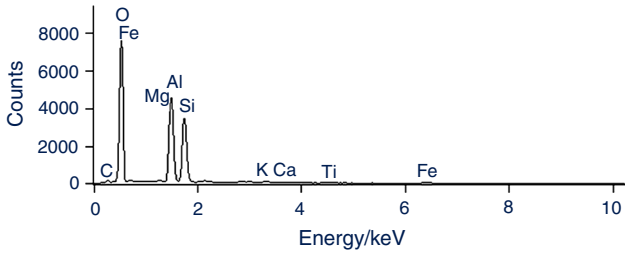

Fig. 2 EDX analysis of G5 proppants sample

$$m_{\mathrm{p}} = 24.7 \times \rho_{\mathrm{bulk}} \tag{5}$$

where ρbulk, a bulk density/g cm^{-3}.

The material should fill the cylinder to specific height so as exerted pressure on a piston's surface averaged 1.95 g cm^{-3}. The falling sample gave a flat surface of material inside the cylinder. The piston was inserted into the cylinder in centric position with reference to the hydraulic press. Force exerted on the piston to obtain

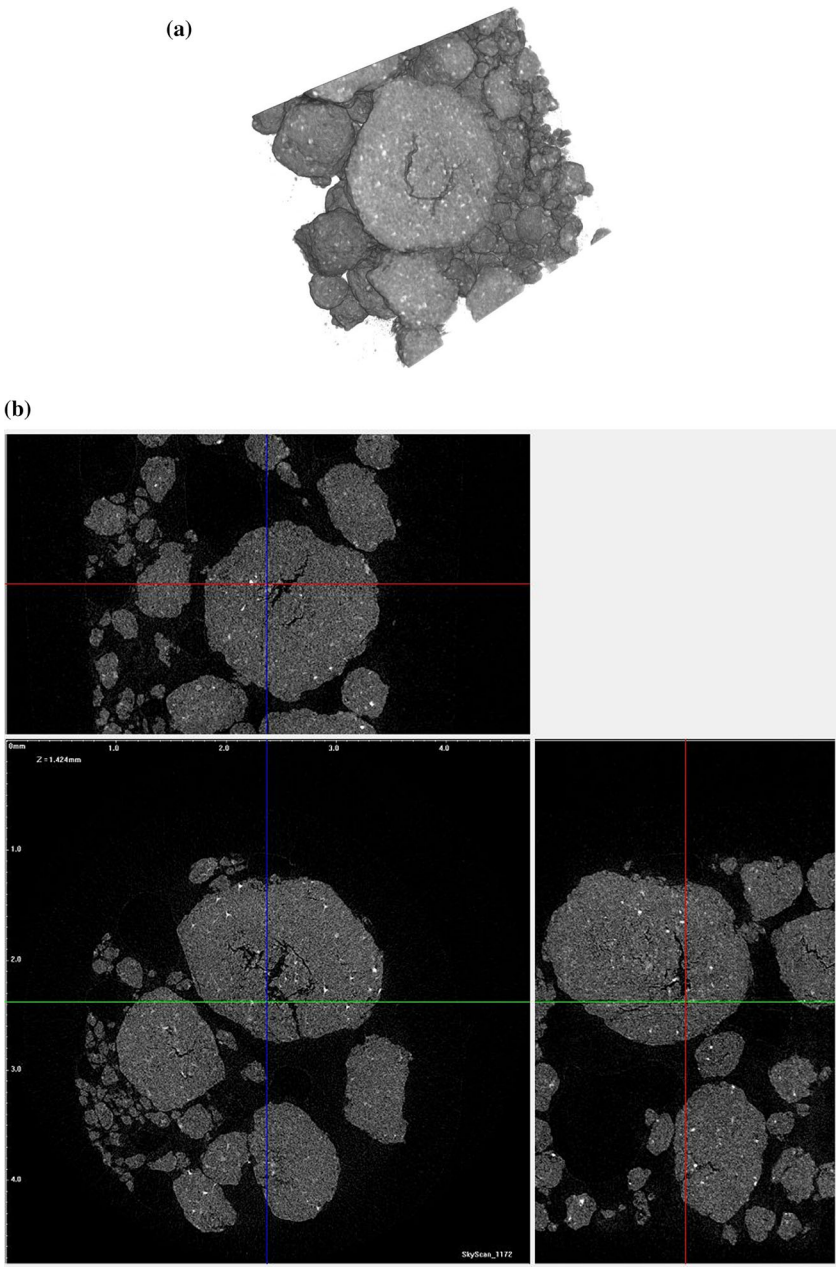

Fig. 3 Tomographic images of G1 proopants: **a** 3D models, **b** interior tomography

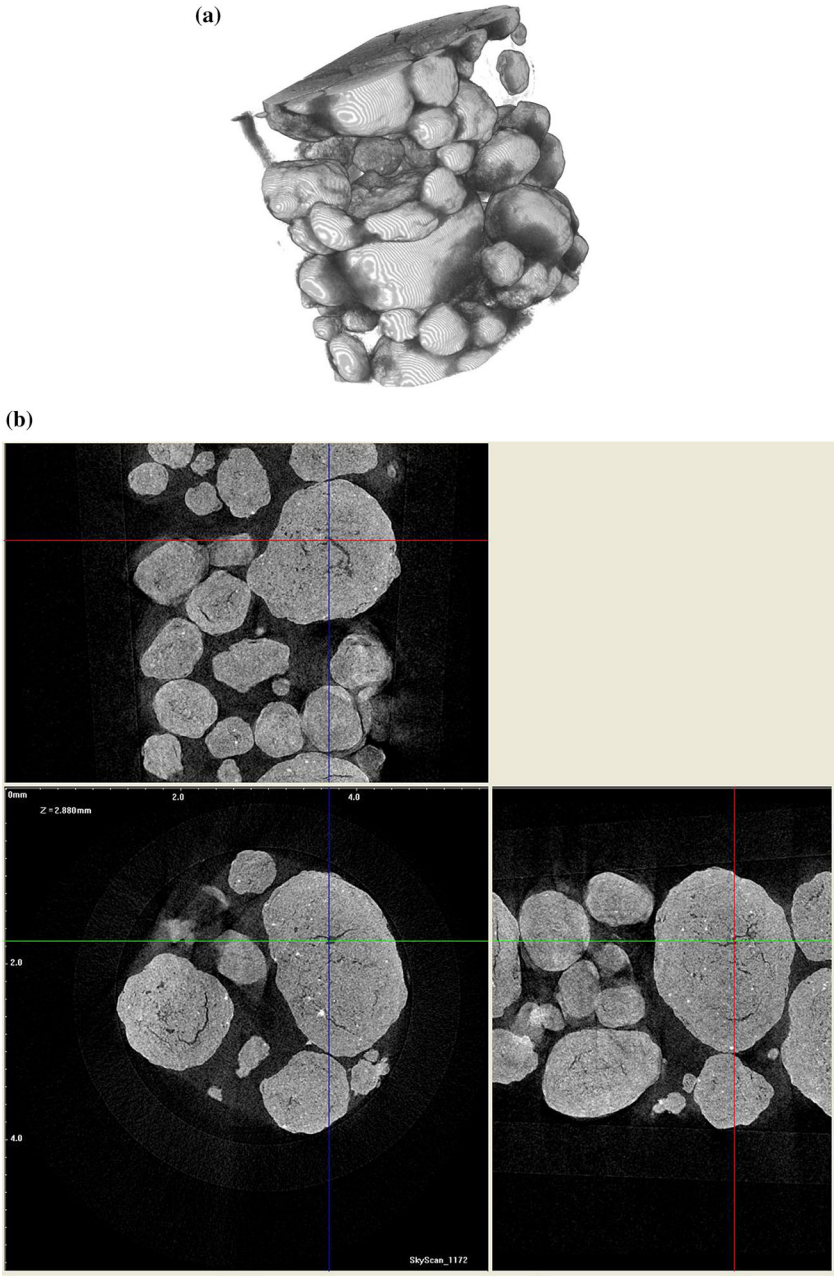

Fig. 4 Tomographic images of G5 proppants: **a** 3D models, **b** interior tomography

required stress values was determined according to Eq. (6):

$$F_{tc} = \frac{\pi \times O\sigma \times d^2 cell}{4} \quad (6)$$

where F_{tc}, force exerted on the piston/N; Ơ, stress exerted on the sample/MPa; d_{cell}, inner diameter of the cylinder/mm.

The force was increasing with a constant speed of increasing piston loading corresponding to growth of the stress (13.8 MPa min^{-1}–2000 psi min^{-1}) up to the final stress value. The stress was maintained for 2 min and then reduced to zero value.

Results and discussion

XRD analysis of raw materials used for the proppants production indicated dominating presence of boehmite and kaolinite, and in minor amounts phases of calcite, anatase, rutile and hematite. Kaolin consists of kaolinite, quartz

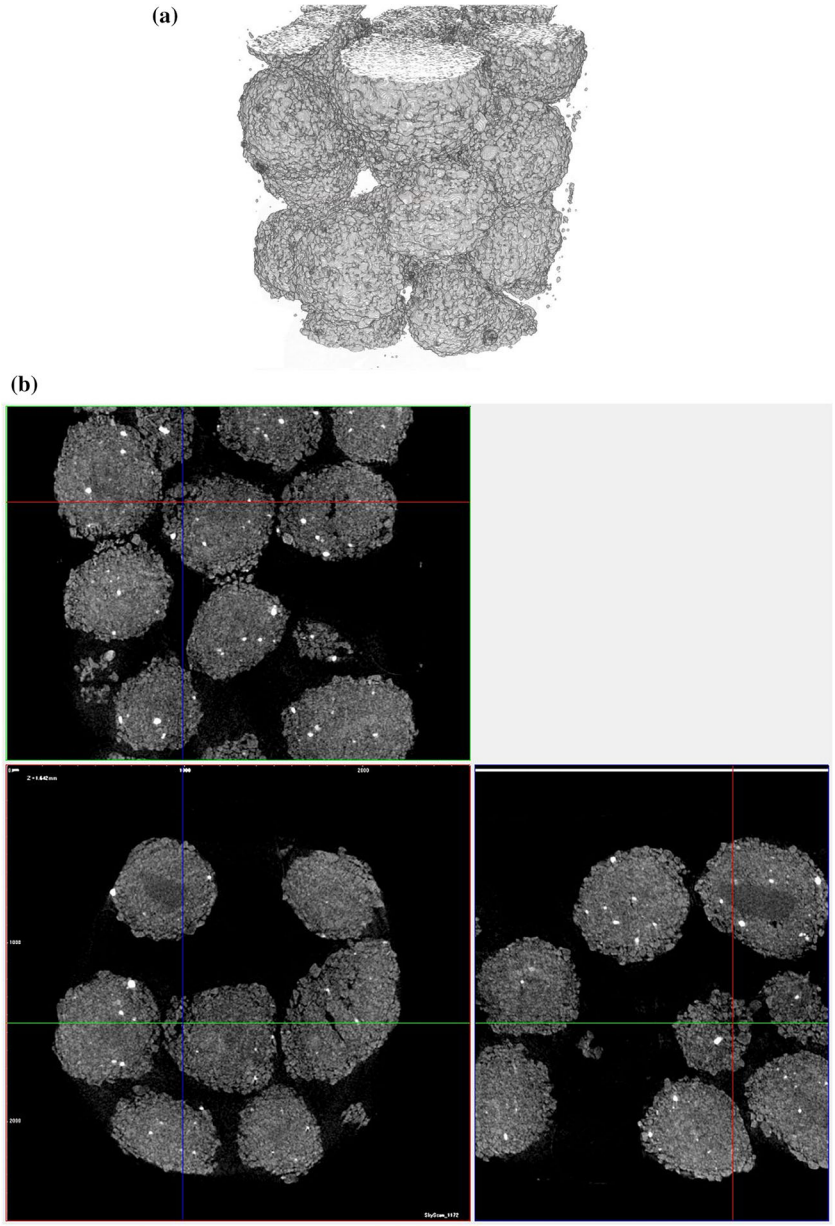

Fig. 5 Tomographic images of 20/40 green proppants, **a** 3D models, **b** interior tomography

alpha and rutile, whereas white clay samples contain kaolinite, potassium calcium aluminum silicate phase, grossite and cristobalit as well.

Obtained granules were differentiated into green proppants (named green pellets: G1, G5) and sintered proppants (named: 16/20 and 20/40) with a chemical content based on the G5 green pellets (addition of poly(acrylic–styrene) dispersion). Analysis of the samples microstructure and their shape were performed by scanning electron microscopy. SEM images (shown in Fig. 1a–h) indicate that there is a difference between all proppants size. G1 (Fig. 1a) demonstrates the smallest diameter, whereas G5 samples (Fig. 1d) exceeds their dimension few times (~0.5 mm). Samples of the investigated green pellets (Fig. 1a–d) are characterized by coarser surface in comparison with the sintered ones (Fig. 1e–h). However, both the green pellets and sintered proppants present similar round shape. The most non-uniform particle size distribution is attributed to G1 proppants (with any polymer addition).

EDS analysis at microareas proved a huge conformity according to chemical content among all studies proppant series. Dominating elements are Al, Si, Mg, Ca, K and Ti that are typical for such kind of materials based on mineral

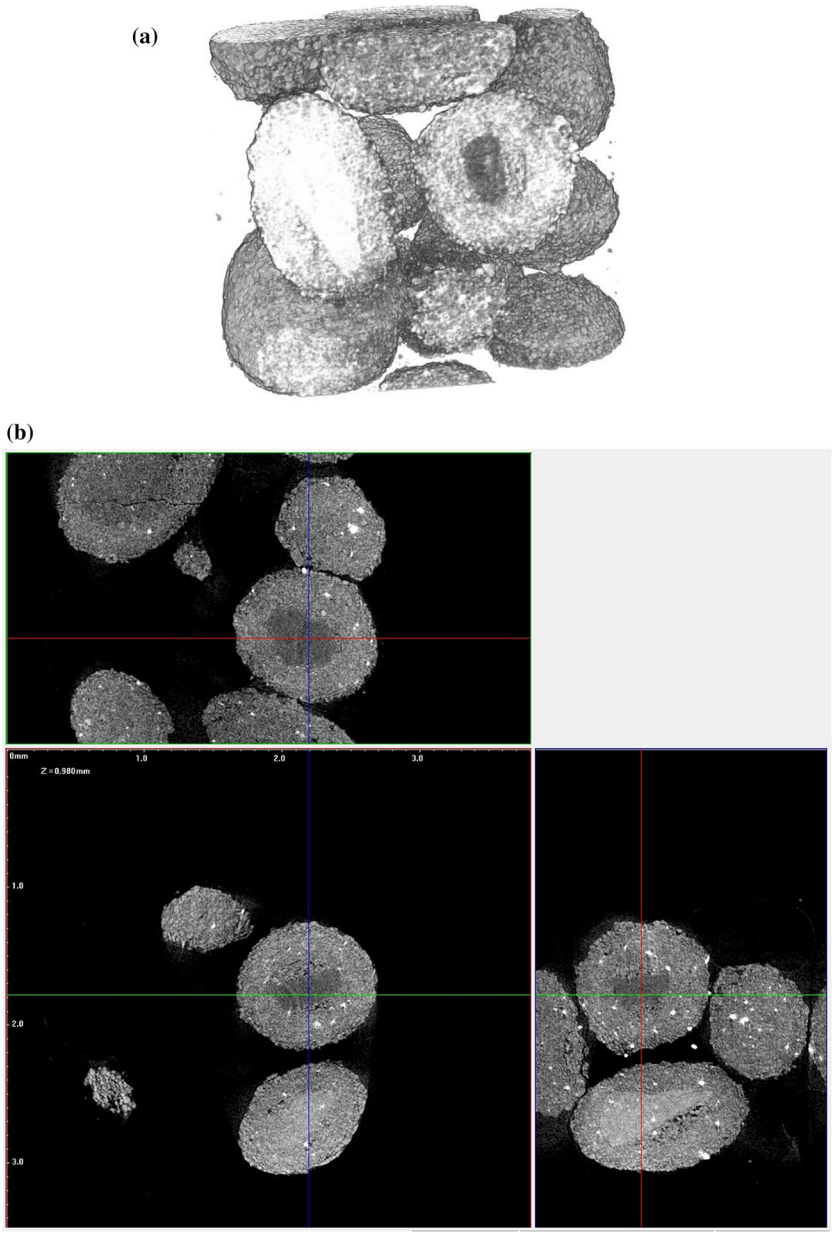

Fig. 6 Tomographic images of 16/20 green proppants, **a** 3D models, **b** interior tomography

raw materials. Presence of Fe suggests the presence of small amount of contaminants taken from mineral deposits (Fig. 2).

Basing on tomographic scanner data, results were subject to reconstruction; thus, propping agent cross sections were obtained. Software designed to ceramic materials analysis provided structure images as the intersection of the *x*, *y*, *z* planes and also 3D models (Figs. 3–8).

G1 green pellets (Fig. 3) demonstrate round shape. However, their size distribution is non-uniform. It has been investigated by many researchers that uniformity of the all kinds of propping agents strictly determines shale gas flow in the reservoir. A minimum 90 % of the settled ceramic granules in the well must be within the specified screen size, as it was discussed in another work [13]. Moreover, the G1 proppants tomography revealed incorrect pores arrangement creating elongated cracks. This is a ground of the substantial risk of insufficient crush resistance of this material in the fracture. These elongated cracks seen in the cross section might lead to the material fracture into fines, blocking a permeability of the fissure. Additionally, a high concentration of the fines corresponds to improper proppants transportation and affects the fracturing fluid rheology. Green proppants with

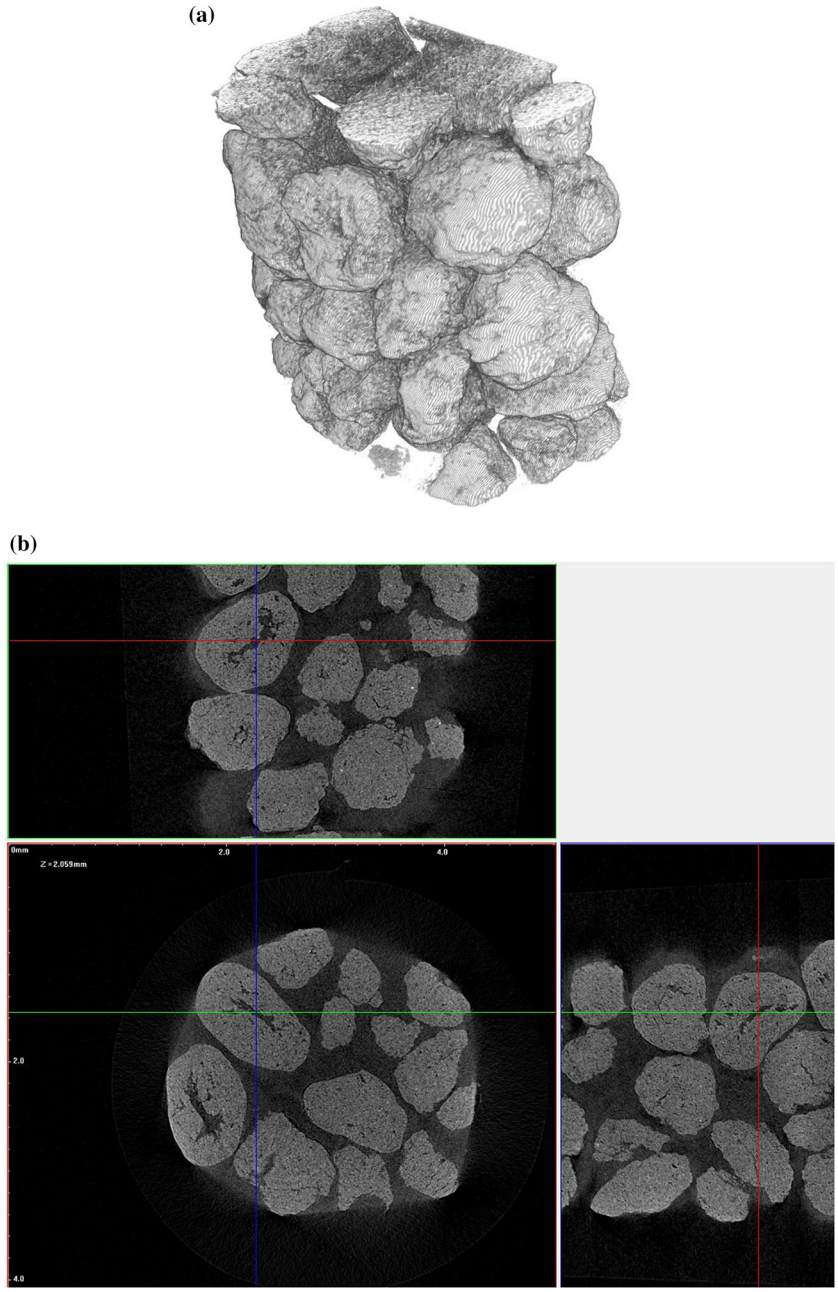

Fig. 7 Tomographic images of 20/40 sintered proppants: **a** 3D models, **b** interior tomography

polymer addition (G5, 16/20, 20/40) perform more uniform size and draw analogy between spheres. However, among the G5 proppants (Fig. 4), there is still an inadmissible distinction in every single granule diameter. This parameter should be as low as possible that rises the material conductivity. The large proppants injected into the wellbore, settle closer blocking the further smaller proppants transportation in a narrow fissure and make them useless. Unfortunately, still there is also a presence of widely arranged macropores inside the material. It is claimed that 50–80 % of pores in propping material cannot be conjoined to assure a proper shale gas flow in a fracture.

The 20/40 (Fig. 5) and 16/20 (Fig. 6) green pellets demonstrate more favorable structure. All of them present a suitable pores geometry and distances between them, which will have an effect on their high mechanical strength after sintering. The 20/40 proppants are smaller than the 16/20 ones (but with similar coarse surface) which means that they can cover a further distance in the fissure and

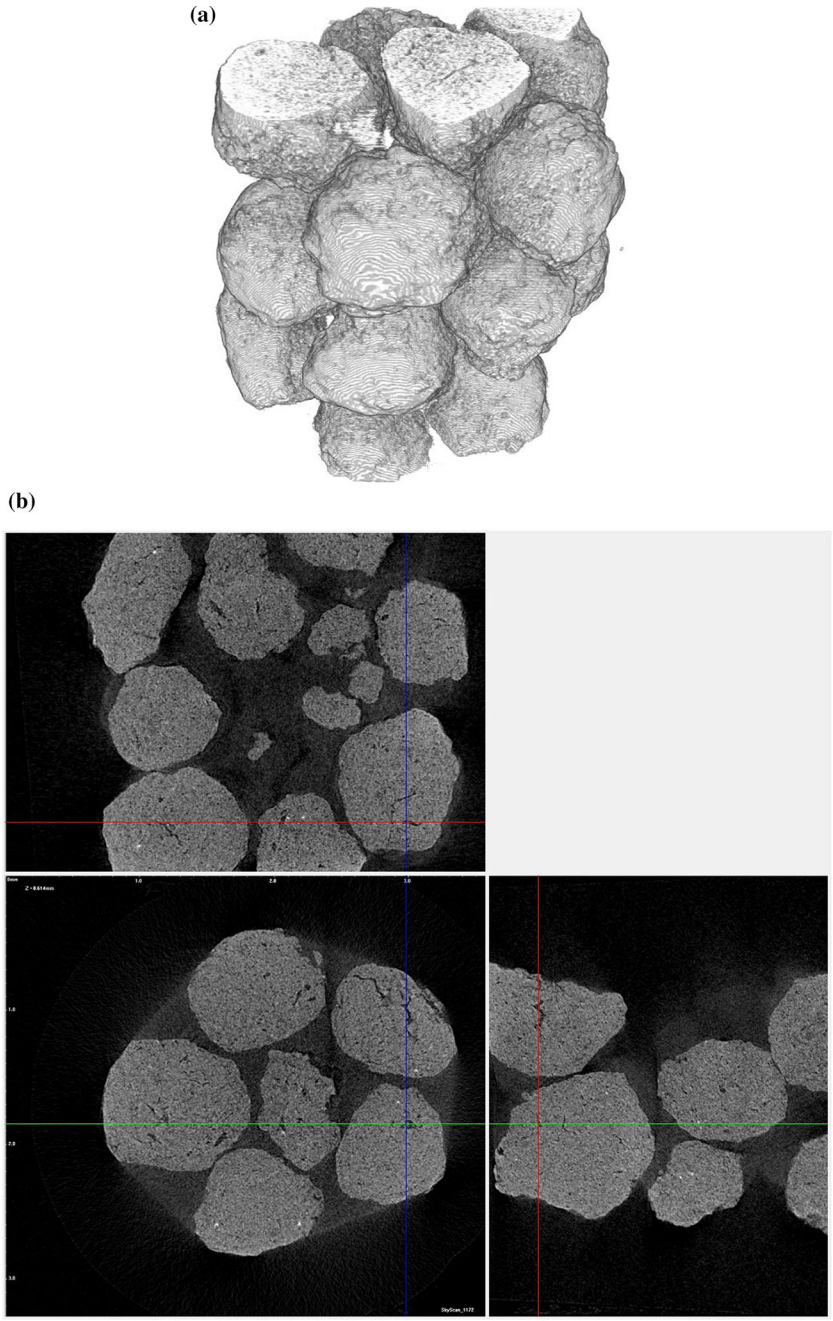

Fig. 8 Tomographic images of 16/20 sintered proppants: **a** 3D models, **b** interior tomography

create a bridge in the embedment. Finally, sintering process affects the regular and small size pores distribution, where best parameters are attributed to the 16/20 sintered granules (Fig. 8). It means that these proppants can be settled in higher amounts and the load will be distributed across more particles. Thus, the large contact angle can reduce tensile stress concentration, assuring a stable prop for the created fracture in the shale formation and finally, enhanced permeability of the material.

Bulk density of the green granules is slightly lower before sintering process (Table 1). According to US 2011/0160104 A1 patent required value of this parameter falls on a range between 1 and 3 g cm^{-3}. All of the samples fulfill this condition.

In Table 2, roundness coefficient of the granules has been compared. Every proppant sample is characterized by required round shape value that results enhanced shale gas conductivity. The highest parameter was obtained for G5 green proppants.

Table 1 Bulk density of ceramic proppants

Proppants	G1	G5	16/20 green	20/40 green	16/20 sintered	20/40 sintered
Bulk density/g cm^{-3}	1.15	1.24	1.08	1.03	1.36	1.34

Table 2 Roundness coefficient of ceramic proppants

Proppants	G1	G5	16/20 green	20/40 green	16/20 sintered	20/40 sintered
Roundness coefficient	0.8	0.87	0.81	0.81	0.81	0.79

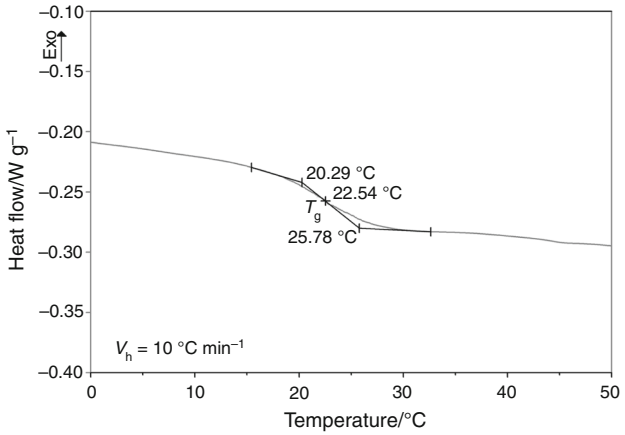

Fig. 9 DSC analysis of poly(acrylic–styrene) dispersion

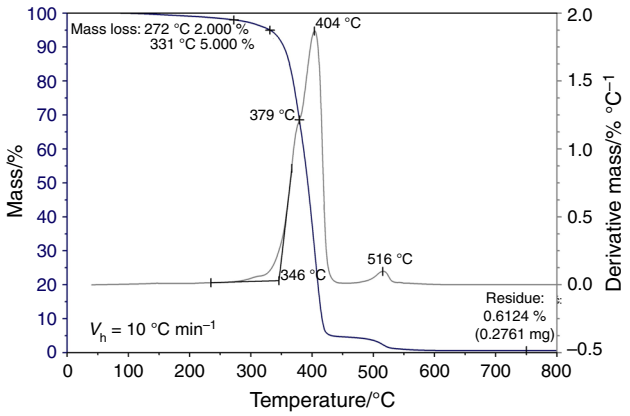

Fig. 10 Mass loss of poly(acrylic–styrene) dispersion as a function of temperature under nitrogen atmosphere—TG and DTG curves

Turbidity value varies from still critical acceptable level: 60. 84 NTU for 16/20 sintered samples to 122 NTU in case of 20/40 proppants. With respect to the Polish water quality norms, drinking water cannot exceed turbidity equal to 1 NTU, while maximum permissible value for proppants comes to 58 NTU. High turbidity value is related to risk of hydraulic fluid contamination by proppants disintegration. It may result with fracture clogging during unconventional gas extraction.

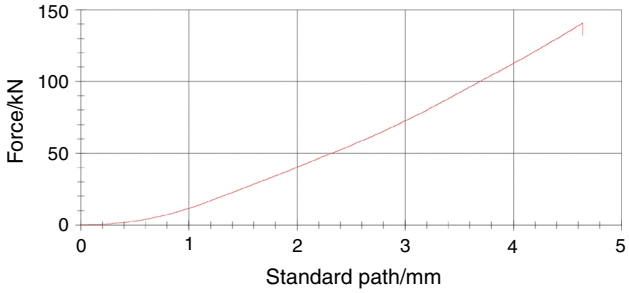

Fig. 11 Crush test results of 20/40 sintered proppants

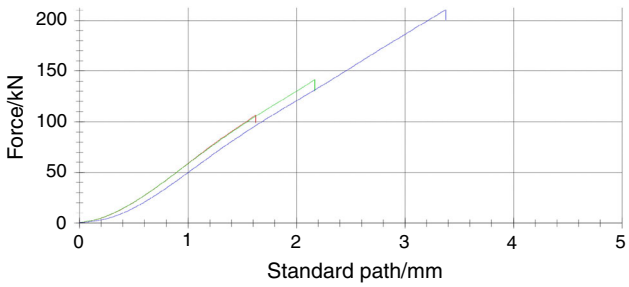

Fig. 12 Crush test results of 16/20 sintered proppants

Both the 16/20 and 20/40 sintered granules demonstrate low susceptibility to acids activity (2.61 and 2.39 %, respectively) where acceptable solubility limit is equal to 7 %.

DSC analysis of the applied water-thinnable poly (acrylic–styrene) dispersion (present in all the samples with the exception of the G1 samples) indicates that copolymer demonstrates low glass transition temperature (T_g) close to the room temperature (as shown in Fig. 9). This value is a consequence of many factors. First of all, there is a lack of groups able to hydrogen bonds formation. Moreover, the presence of a phenyl group, which acts as "a stiff group," causes reducing of the copolymer rotation and therefore raising T_g value to the room temperature [26]. What is more, an irregular structure of the copolymer chain and increase in a length of aliphatic radicals lowers T_g due to increased rotation energy of a single particle around the bonds in the main chain. Therefore, there occurs

simultaneously increase in plasticity of polymer that behaves as amorphous material. The sufficiently low T_g value and the presence of suitable functional groups in the copolymer ensure good cohesion of polymer dispersion separately and adhesion of the copolymer to the powder grains surface as well. Such a relation prevents the formation of raw materials agglomerates. All these parameters correspond to wettability of the powder by the polymer, and thus the strength of the final sintered proppants owing to the ceramic filler–copolymer interface. The estimated glass transition temperature is much lower than proppants granulation (40 °C) and the sintering temperature; thus, there is no need to add plasticizers to the initial raw mixture. What is more, the final sintered material demonstrates high mechanical strength.

The thermal decomposition of the polymers can take place in few stages. It was examined that the polymer degradation due to thermal exposition is dependent on its chemical structure. This phenomenon is initiated by the decomposition of the weakest bonds at the temperature specific for every compound corresponding to the presence of the diverse groups attached to the main chain. Usually, this temperature value is related to the 5 % mass loss. In case of the examined copolymer (poly(acrylic–styrene), the initial degradation relates to drop in the mass of 2 %, noticed for 272 °C which is a result of macromonomers release from the end chains. The rapid material degradation (5 % mass loss) started at 331 °C (presented in Fig. 10) where the polymer fragments with high activity (and thus low activation energy) decomposed first in the dispersion. The sharp change in the mass is observed to 425 °C, leaving 7 % of the mass sample, corresponding to the continuous decomposition into monomers and side chains containing phenyl groups. Further slower copolymer decomposition occurs in the temperature range of 425–523 °C (98 % of mass loss), expected for unbranched hydrocarbon chains. The last, in trace amounts, mass loss step is observed between 523 and 600 °C. The copolymer behaves as thermal stable at 600 °C with the final mass of 0.2761 mg. It corresponds to the general 99.3876 % decomposition of the copolymer for the whole heating process. The remaining mass may relate to the part of impurities that could not be removed from the polymer. The results calculated from the DTG curve (Fig. 10) revealed that the dynamics of the degradation proceeds between 346 and 516 °C. The onset temperature (T_{onset}) for the thermal degradation of the poly (acrylic–styrene) dispersion is noticed at 404 °C, which indicates a rapid decomposition into monomers. According to the DTG data, the definitely slower thermal degradation occurs also at 516 °C, verified as a new small peak in the temperature range between 450 and 530 °C. It can be attributed to the defragmentation of additional bonds or groups in the material.

Conducted crush tests proved that 16/20 proppant series are more resistant to mechanical strength in comparison with 20/40 granules (Figs. 11, 12) which is related to the pores size and distribution inside the material. A total of 16/20 proppants were able to resist even in the highest stress of 210 kN (103 MPa–15,000 psi), whereas 20/40 series crushed after 4 min of exerted pressure (51.71 MPa–105.5 kN–7500 psi).

Conclusions

Results of conducted research studies indicate that raw materials used to proppants production consist of compounds typical for loamy deposits where Al_2O_3 and SiO_2 are dominating compounds. All of the proppants demonstrate proper roundness coefficient, whereas the most uniform shape reveal the 20/40 and 16/20 proppant samples. The studied granules are characterized by slightly coarse surface. The regular pores arrangement is characteristic for the 16/20 sintered samples which results in their high mechanical strength. The 20/40 granules perform insufficient resistivity to high stress values; thus, there is a risk of these proppants will flatten and pack together under high closure stresses during shale gas extraction.

The sintered proppants are stable in strong acidic environment. However, the 20/40 proppants are prone to disintegration in water making a risk of fracture clogging and a straitened gas flow. All the samples are characterized by low thus bulk density that results in their facilitated transport in liquid medium.

The glass transition temperature analysis was a very crucial part of the polymeric binder investigation and enabled determination of its impact on the rheological properties of applied powders as well as the critical parameters of the ceramic materials obtained with them. The implemented copolymer dispersion (to G5, 16/20 and 20/40 proppants) demonstrates the low glass transition; thus, the sintered propping agents perform increased mechanical strength. What is more, T_g value nearly equal to the room temperature also influences the manufacturing costs, because there is no need to add other dispersants lowering the binder T_g value.

The thermal decomposition results obtained by thermogravimetry method reveal the material is prone to thermal degradation starting at 272 °C. Further exposition to 600 °C causes almost total material degradation, where is only 0.6124 % material residue. The TG and DTG curves data indicate that the poly(acrylic–styrene) dispersion can be applied as a binder in the initial proppants manufacturing (granulation process), where is functional and thermal stable.

To sum up, the investigated light ceramic proppants perform properties which enable their application for

hydraulic fracturing in strict geological conditions determined by extremely high pressure, temperature and low permeability of shale formations. The granules fulfill the norms and thus state a prospective material on a global proppants market.

Acknowledgements Financial support of BLUE GAS Programme financed from The National Centre for Research and Development Project: "Optimizing the lightweight high strength and low specific gravity ceramic proppants production technology maximally using naturally occurring Polish raw materials and fly ash," No. BG1/BALTICPROPP/13 is gratefully acknowledged.

References

1. Osikowicz R. Paliwa i Energetyka. Rynek gazu na świecie. Mar 2012.
2. Woźniak P, Janus D. Gaz z łupków, szczelinowanie i ceramiczne proppanty cz. 1. Wiadomości. 2013;3:7–12.
3. BP. BP Energy Outlook 2035. 2014. http://www.bp.com/content/dam/bp/pdf/energy-economics/energy-outlook-2016/bp-energy-outlook-2014.pdf. Accessed Apr 2014.
4. Przybylik M, Stangierski P, Oswald K. Paliwa i Energetyka. Apr 2013.
5. Baltic Ceramics. Memorandum. Warsaw University of Technology; 2012.
6. Woźniak P, Janus D. Jaki proppant jest każdy widzi—czyli o metodach wyznaczania parametrów charakterystycznych i o producentach. Wiadomości. 2013;8:14–8.
7. Woźniak P, Janus D. Gaz z łupków, szczelinowanie i ceramiczne proppanty cz. 2. Wiadomości. 2013;4:13–8.
8. Beckiwith R. Proppants: Where in the world. 2011.
9. Ciechanowska M, Kasza P, Lubaś J, Matyasik I, Such P. Instytut Nafty i Gazu. Raport nt. Uwarunkowania rozwoju wydobycia gazu z polskich formacji łupkowych. Forum Energetyczne. Sopot: 2012.
10. Schlumberger. High pressure, High temperature (HPHT), 2014; http://www.slb.com/services/technical_challenges/high_pressure_high_temperature.aspx. Accessed 15 Oct 2015.
11. Don L. Proppants open production Pathways. 2011. https://www.slb.com/~/media/Files/stimulation/industry_articles/201101_ep_proppant_design.ashx. Accessed 20 Apr 2014.
12. Richerson DW. Modern ceramic engineering: properties, processing and use in design. 3rd ed. CRC Press; 2006. p. 29.
13. Szymanska J, Wisniewski P, Wawulska-Marek P, Malek M, Mizera J. Selecting key parameters ot the green pellets and lighweight ceramic proppants for enhanced shale gas exploitation. Procedia Struct Integr. 2016;1:297–304.
14. Ottestad E. Proppants, properties and Requirement. NTNU. 2013.
15. Wisniewski P, Szymanska J, Malek M, Mizera J. Optimizing the lightweight ceramic proppants properties. Acta Phys Pol, A. 2016;129:501–3.
16. Szymanska J. Studies of the lightweight ceramic proppants using naturally occurring Polish raw materials. MSc Thesis. Warsaw University of Technology; 2014.
17. Wisniewski P, Malek M, Szymanska J, Zarzycka-Dziedzic D, Mizera J, Kurzydlowski KJ. Studies on receiving ceramic proppants by the spray drying method. Ceram Mater. 2015;67:448–53.
18. Pratap A, Sharma K. Applications of some thermo-analytical techniques to glasses and polymers. Budapest. 2012;107:171–82. doi:10.1007/s10973-011-1816-y.
19. Zhouyue L, Wang X, Jinrong W, Guangsu H, Xiaoan W, Lijuan Z. The proper glass transition temperature of amorphous polymers on dynamic mechanical spectra. J Therm Anal Calorim. 2013;116:447–53. doi:10.1007/s10973-013-3526-0.
20. Fueglein E, Kaisersberger E. About the development of databases in thermal analysis. J Therm Anal Calorim. 2015;120:23–31. doi:10.1007/s10973-014-4381-3.
21. Szafran M, Wisniewski P, Rokicki G. Effect of glass transition temperature of polymeric binders on properties ceramic material. J Therm Anal Calorim. 2004;77:319–27.
22. Wisniewski P. Badania nad procesem prasowania tlenku glinu z udziałem nowych wodorozcieńczalnych spoiw polimerowych. PhD Thesis. Warsaw University of Technology, 2003.
23. Rodríguez Martínez AD, Domínguez Patiño ML, Melgoza Alemán RM, Rosas Trejo GA. Characterization by thermogravimetric analysis of polymeric concrete with high density polyethylene mechanically recycled. J Miner Mater Charact Eng. 2014;2:259–63.
24. Zhang T, Howell BA, Smith PB. Thermal degradation of carboxy-terminal trimethylolpropane/adipic acid hyperbranched poly(ester)s. J Therm Anal Calorim. 2015;122:1159–66. doi:10.1007/s10973-015-4790-y.
25. Zhang GZ, Zhang J, Wang F, Li HJ. Thermal decomposition and kinetics studies on the poly (2,2-dinitropropyl acrylate) and 2,2-dinitropropyl acrylate-2,2-dinitrobutyl acrylate copolymer. J Therm Anal Calorim. 2015;122:419–26. doi:10.1007/s10973-015-4687-9.
26. Maciejewska M. Synthesis and characterization of textural and thermal properties of polymer monoliths. J Therm Anal Calorim. 2015;121:1333–43. doi:10.1007/s10973-015-4538-8.
27. Zhang GZ, Zhang J, Li HJ, Zhao S. Synthesis and thermal behavior of *gem*-dinitro valerylated olystyrene. J Therm Anal Calorim. 2014;. doi:10.1007/s10973-014-3840-1.